

# Mixed convection in wall plumes

RAMESH KRISHNAMURTHY and BENJAMIN GEBHART

Department of Mechanical Engineering and Applied Mechanics, University of Pennsylvania,  
 Philadelphia, PA 19104, U.S.A.

(Received 9 June 1983 and in revised form 22 November 1983)

**Abstract**—An analysis is presented for mixed convection effects in a wall plume flow. The results apply downstream from the source. The method of matched asymptotic expansions has been used to obtain a consistent solution by simultaneously including both the effects of mixed convection and of higher order boundary layer corrections. Several subtle and interesting features of this flow arise and are explained. The unexpected role played by Prandtl number is clearly illustrated. For example, the effect of an aiding imposed forced flow is to reduce surface shear stress, for  $Pr = 0.7$ , and to increase it for  $Pr = 6.7$ . Further, it has been shown that such a Prandtl number effect on the surface shear stress is dependent on the kind of heating condition imposed at the surface. Results of numerical calculations are presented for two values of Prandtl number, 0.7 and 6.7, as characteristic of air and water, respectively. The overall effect of mixed convection on the downstream decay of surface temperature and on the maximum value of tangential velocity is seen to be greater in air than in water.

## INTRODUCTION

THE FLOW resulting from a horizontal line source of heat imbedded at the base of a vertical adiabatic surface, with the ambient fluid moving with a uniform velocity, is considered here. The same circumstance with the ambient fluid at rest is conventionally referred to as the convective plane wall plume. The similarity solution for the convective wall plume has been studied earlier by Zimin and Lyakhov [1] and also by Jaluria and Gebhart [2]. Higher order corrections to account for the nonboundary layer effects in a wall plume were given by Afzal [3]. The mixed convection flow over a wide horizontal heated element of finite height, located on a vertical adiabatic surface in an external, aiding flow was analyzed by Jaluria [4]. In a wall plume, the vertical component of the velocity  $u$  (see Fig. 1), increases as  $x^{1/5}$ ,  $x$  being the distance downstream of the heat source. Thus, even in the presence of an appreciable free stream velocity,  $U_\infty$ , at sufficiently large values of  $x$ , the buoyancy effect will dominate the transport mechanism. The situation considered here is that of a small mixed convection effect or free stream flow, in the same direction as the buoyancy force arising from the horizontal line source. This circumstance is of considerable interest in many manufacturing processes and is of particular relevance to cooling of components in electronic circuitry.

The effect of nonzero free stream velocity is considered as a perturbation of the buoyancy induced wall plume. It is mathematically appropriate to construct the perturbation expansions taking the boundary layer equations as the governing equations. However, from a physical standpoint, as pointed out by Carey and Gebhart [5], the second order contributions of the terms pertaining to mixed convection may be of comparable magnitude to the contributions of terms discarded in establishing the boundary layer equations, from the Navier–Stokes equations. Thus, in order to

obtain a consistent solution, the effects of mixed convection and of higher order boundary layer corrections must be considered simultaneously. The first such simultaneous and consistent assessment of mixed convection effects was the analysis given by Carey and Gebhart [5]. The method of matched asymptotic expansion is used here to obtain a solution valid at large downstream distance from the source. Two perturbation parameters,  $\varepsilon_H$  and  $\varepsilon_M$ , characterize the boundary layer corrections and the effects of nonzero free stream velocity, respectively. These two effects are considered simultaneously for a wall plume. Numerical results are given for  $Pr = 0.7$  and 6.7. Two types of thermal conditions at the surface are considered. In one, the surface is taken to be completely adiabatic and in the other the downstream surface temperature distribution is so prescribed that it is adiabatic to the zero order only. This is done in order to examine the effect of the surface thermal condition on the various flow characteristics such as surface shear stress, etc.

## ANALYSIS

The mixed convection flow arising from an infinitely long horizontal line source of heat embedded in the base of a vertical adiabatic surface is considered here, as a steady, plane flow. The coordinates and velocity variables are defined in Fig. 1. Invoking the Boussinesq approximations and neglecting the effects of viscous dissipation and pressure in the energy equation, the complete two dimensional governing equations take the form

$$\begin{aligned} \psi_y \frac{\partial}{\partial x} (\psi_{xx} + \psi_{yy}) - \psi_x \frac{\partial}{\partial y} (\psi_{xx} + \psi_{yy}) \\ - \nu \nabla^4 \psi - g\beta \frac{\partial t}{\partial y} = 0 \quad (1) \end{aligned}$$

## NOMENCLATURE

$A_i$	constants, defined in equations (16a)–(16d) and (20c) ( $i = 0, 1, 2, 3, 4$ )
$C_n$	constants associated with eigenfunctions of the inner expansion ( $n = 1, 2, \dots$ )
$C_p$	specific heat
$D$	$(g\beta N/4\nu^2)^{-5/12}$
$f_n$	eigenfunctions of the inner expansions for the stream function $\psi$ ( $n = 1, 2, \dots$ )
$F_i$	terms in the inner expansion of the stream function $\psi$ ( $i = 0, 1, 2, 3, 4$ )
$g$	acceleration due to gravity
$G$	$4(Gr_x/4)^{1/4}$
$G_i$	terms in the inner expansion of $H$ ( $i = 3, 4$ )
$Gr_x$	$(gx^3/\nu^2)\beta\Delta T$
$H$	$(t-t_\infty)/\Delta T$
$H_i$	terms in the inner expansion of $H$ ( $i = 0, 1, 2, 3, 4$ )
$I_0$	$\int_0^\infty F'_0 H_0 \, d\eta$
$J_i$	terms in the inner expansion of the stream function $\psi$ ( $i = 3, 4$ )
$k$	thermal conductivity
$N$	$[Q_0^4/g\beta\rho^2\mu^2C_p^4I_0^4]^{1/5}/4$
$Pr$	Prandtl number
$Q$	local thermal convected energy in the boundary layer
$Q_0$	thermal input per unit length of the line source
$r$	radial polar coordinate measured from the heat source

$\bar{R}$	$2U_\infty/\nu[4Pr I_0 k\nu^2/g\beta Q_0]^{1/3}$
$Re_x$	$U_\infty x/\nu$
$t$	temperature
$t_0$	surface temperature
$t_\infty$	ambient temperature
$\Delta T$	$Nx^{-3/5}$
$u$	velocity in the $x$ -direction
$U_\infty$	free stream velocity
$v$	velocity in the $y$ -direction
$x$	coordinate parallel to the surface
$y$	coordinate normal to the surface.

## Greek symbols

$\beta$	coefficient of thermal expansion
$\varepsilon_H$	$[Gr_x/4]^{-1/4}$
$\varepsilon_M$	$4Re_x/G^2$
$\eta$	$yG/4x$
$\theta$	$(t-t_\infty)$ in the inner expansion
$\bar{\theta}$	$(t-t_\infty)$ in the outer expansion
$\lambda_n$	eigenvalues associated with $f_n$ and $\phi_n$
$\mu$	coefficient of viscosity
$\nu$	kinematic viscosity
$\rho$	density
$\phi$	$\tan^{-1}(y/x)$
$\phi_n$	eigenfunction associated with the inner expansion for $\theta$
$\psi$	stream function
$\bar{\psi}$	stream function in the outer expansion
$\bar{\psi}_i$	terms in the expansion for $\bar{\psi}$ ( $i = 1, 2, \dots$ ).

and

$$\psi_y \frac{\partial t}{\partial x} - \psi_x \frac{\partial t}{\partial y} = \frac{\nu}{Pr} (t_{xx} + t_{yy}) \quad (2)$$

where the stream function  $\psi$  has been defined so that

$$u = \psi_y \quad \text{and} \quad v = -\psi_x.$$

Here  $t$  represents the temperature,  $\nu$  the kinematic viscosity,  $g$  the acceleration due to gravity,  $\beta$  the volumetric coefficient of thermal expansion and  $Pr$  the Prandtl number. Boundary conditions are

$$x > 0, y = 0, \quad \psi = \psi_y = t_y = 0 \quad (3a)$$

$$y \rightarrow \infty, \quad \psi_y \rightarrow U_\infty, t \rightarrow t_\infty \quad (3b)$$

$$x \leq 0, y = 0, \quad \psi = \psi_{yy} = t_y = 0. \quad (3c)$$

Also, for  $x > 0$ , for an adiabatic surface, the total convected energy downstream remains constant

$$Q(x) = \int_0^\infty \rho c_p \psi_y (t - t_\infty) \, dy = Q_0 = \text{const.} \quad (4)$$

where  $Q_0$  is the thermal input per unit length of the line source,  $\rho$  is the density and  $c_p$  is the specific heat.

The two perturbation parameters which arise are  $\varepsilon_M$ , characterizing mixed convection effects, and  $\varepsilon_H$ , the higher order boundary layer corrections.  $\varepsilon_H$  represents the effects of the terms neglected in deriving the boundary layer equations from the Navier–Stokes equations. The inner and outer expansions are then taken as follows:

$$\begin{aligned} \psi = 4\nu \left( \frac{Gr_x}{4} \right)^{1/4} & [F_0(\eta) + \varepsilon_M F_1(\eta) \\ & + \varepsilon_M^2 F_2(\eta) + \varepsilon_M^3 F_3(\eta) + \varepsilon_H J_3(\eta) \\ & + \varepsilon_M^4 F_4(\eta) + \varepsilon_M \varepsilon_H J_4(\eta) + \dots] \end{aligned} \quad (5)$$

$$\begin{aligned} \theta = t - t_\infty = \Delta T & [H_0(\eta) + \varepsilon_M H_1(\eta) + \varepsilon_M^2 H_2(\eta) \\ & + \varepsilon_M^3 H_3(\eta) + \varepsilon_H G_3(\eta) + \varepsilon_M^4 H_4(\eta) \\ & + \varepsilon_M \varepsilon_H G_4(\eta) + \dots] \end{aligned} \quad (6)$$

Outer

$$\bar{\psi} = \bar{\psi}_0 + \bar{\psi}_1 + \bar{\psi}_2 + \bar{\psi}_3 + \dots \quad (7)$$

$$\bar{\theta} = t - t_\infty = 0 \quad (8)$$

where  $\Delta T = Nx^{-3/5}$  represents the local temperature

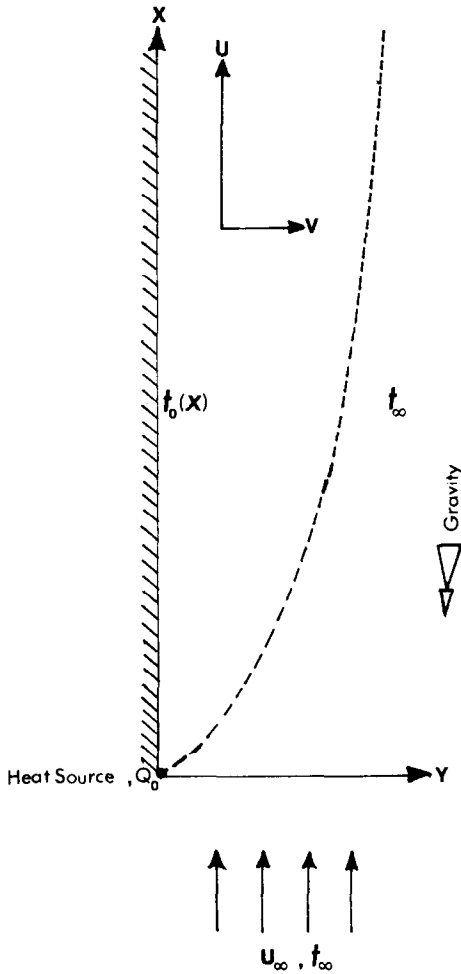


FIG. 1. Geometry.

difference  $(t_0 - t_\infty)$ , between the surface and the ambient, resulting from the zero order boundary layer solution. This solution is  $F_0$  and  $H_0$  for the velocity and temperature fields, respectively

$$Gr_x = \frac{gx^3\beta\Delta T}{\nu^2} = \left(\frac{g\beta N}{\nu^2}\right)x^{12/5};$$

$$\eta = \frac{y}{x}(Gr_x/4)^{1/4} = \frac{y}{4x}G$$

$$N = \left[\frac{Q_0^4}{4^5 g\beta\rho^2\mu^2 c_p^4 I_0^4}\right]^{1/5}; \quad I_0 = \int_0^\infty F_0 H_0 d\eta$$

and  $\mu$  is the viscosity.

The choice of  $\varepsilon_M$  is made so that  $F_0$  and  $H_0$  are the solutions of the natural convection boundary layer flow of a wall plume. To this end the first of the boundary conditions in equation (3b) is rewritten as

$$u = \psi_y = 4\nu\left(\frac{Gr_x}{4}\right)^{1/4} F_0'(\eta) \frac{1}{x} \\ \times \left(\frac{Gr_x}{4}\right)^{1/4} \rightarrow U_\infty, \quad \text{as } y \rightarrow \infty$$

that is

$$\frac{4\nu}{x}\left(\frac{Gr_x}{4}\right)^{1/2} F_0'(\infty) \rightarrow U_\infty$$

and

$$F_0'(\infty) \rightarrow \frac{1}{4}\left(\frac{U_\infty x}{\nu}\right) \left/\left(\frac{Gr_x}{4}\right)^{1/2}\right. \\ = \frac{1}{4} Re_x \left/\left(\frac{Gr_x}{4}\right)^{1/2}\right. = 4 Re_x / G^2.$$

Hence  $\varepsilon_M$  is chosen to be  $Re_x/[Gr_x/4]^{1/2}$ . Following Yang and Jerger [6],  $\varepsilon_H$  is chosen as  $[Gr_x/4]^{-1/4}$ . This value arises from a consideration of the order of magnitude of the normal velocity component at the outer edge of the boundary layer flow as calculated from the zero order boundary layer solution. Then  $\varepsilon_H$  and  $\varepsilon_M$  are related as

$$\varepsilon_M = \bar{R}\varepsilon_H^{1/3} \quad \text{where} \quad \bar{R} = \frac{2U_\infty}{\nu}\left(\frac{4Pr I_0 k\nu^2}{g\beta Q_0}\right)^{1/3}.$$

For some ordinary values of  $Q_0$  and  $U_\infty$  encountered ( $Q_0 \sim 50 \text{ W m}^{-1}$ , and  $U_\infty \sim 1\text{--}10 \text{ cm s}^{-1}$ )  $\bar{R}$  is a constant of the order of unity.

Expansions (5) and (6) are then substituted into the governing equations (1) and (2). Perturbation equations are then obtained by collecting like powers of  $\varepsilon_M$ ,  $\varepsilon_H$  and  $\varepsilon_M\varepsilon_H$ . It is noted that, in the inner expansion, the terms of  $O(\varepsilon_M^3)$  and  $O(\varepsilon_H)$  must be taken as distinct, although it may be mathematically appropriate to combine them into one term, since both are proportional to  $x^{-3/5}$  if  $\bar{R} = O(1)$ . These two terms result from physically distinct higher order effects. They do not interact with each other at this level of the expansion. For similar reasons, the terms of  $O(\varepsilon_M^4)$  and  $O(\varepsilon_M\varepsilon_H)$  are taken as distinct. This situation is peculiar to the plume [7] and to a wall plume. Such a circumstance was not encountered by Carey and Gebhart [5] in the calculation of the mixed convection flow adjacent to a vertical surface dissipating heat uniformly.

Employing the usual asymptotic matching techniques, boundary conditions are obtained for each level of expansion in the inner and outer regions. As mentioned before, for a wall plume, the vertical surface may be considered as adiabatic downstream or as being maintained at a temperature distribution  $t_0(x)$  such that it is adiabatic to the zero order only. While both the possibilities are considered, for the sake of brevity, only the equations corresponding to the adiabatic surface are listed below. The primes denote derivatives with respect to  $\eta$ . Then after matching it is found that the terms of inner expansion up to  $O(\varepsilon_M\varepsilon_H)$  must satisfy

$$F_0''' + \frac{12}{5}F_0 F_0'' - \frac{4}{5}F_0'^2 + H_0 = 0 \quad (9a)$$

$$H_0'' + \frac{12}{5}Pr(F_0 H_0)' = 0 \quad (9b)$$

$$F_0(0) = F_0'(0) = F_0'(\infty) = H_0(0) - 1 = H_0'(0) = 0 \quad (9c)$$

$$F_1''' + \frac{4}{5}(3F_0F_1'' + 2F_1F_0'' - F_1'F_0') + H_1 = 0 \quad (10a)$$

$$H_1'' + \frac{4}{5}Pr(3F_0H_1' + 2F_1H_0' + 4H_1F_0' + 3H_0F_1') = 0 \quad (10b)$$

$$F_1(0) = F_1'(0) = F_1'(\infty) - \frac{1}{4} = H_1'(0) = H_1(\infty) = 0 \quad (10c)$$

$$F_2''' + \frac{4}{5}(3F_0F_2'' + 2F_1F_1'' + F_0''F_2) + H_2 = 0 \quad (11a)$$

$$H_2'' + \frac{4}{5}Pr(F_2H_0' + 2F_1H_1' + 3F_0H_2' + 5F_0'F_2 + 4H_1F_1' + 3H_0F_2') = 0 \quad (11b)$$

$$F_2(0) = F_2'(0) = F_2'(\infty) = H_2'(0) = H_2(\infty) = 0 \quad (11c)$$

$$F_3''' + \frac{4}{5}(F_2F_1'' + F_1'F_2' + 2F_1F_2'' + 3F_0F_3'' + F_0'F_3') + H_3 = 0 \quad (12a)$$

$$H_3'' + \frac{4}{5}Pr(3F_0H_3' + 2F_1H_2' + F_2H_1' + 6H_3F_0' + 5F_1'F_2 + 4H_1F_2' + 3H_0F_3') = 0 \quad (12b)$$

$$F_3(0) = F_3'(0) = F_3'(\infty) = H_3'(0) = H_3(\infty) = 0 \quad (12c)$$

$$J_3'' + \frac{4}{5}(3F_0J_3'' + F_0'J_3') + G_3 = 0 \quad (13a)$$

$$G_3'' + \frac{4}{5}Pr(3F_0G_3' + 6G_3F_0' + 3H_0J_3') = 0 \quad (13b)$$

$$J_3(0) = J_3'(0) = J_3'(\infty) - \frac{3}{5}A_0 \cot\left(\frac{2\pi}{5}\right) \times \left(\frac{2\pi}{5}\right) = G_3'(0) = G_3(\infty) = 0 \quad (13c)$$

$$F_4''' + \frac{4}{5}(2F_4'F_0' - F_0''F_4 + 3F_0F_4'' + F_2'F_2' + (F_2')^2 + 2F_1'F_3' + 2F_3'F_1') + H_4 = 0 \quad (14a)$$

$$H_4'' + \frac{4}{5}Pr(-F_4H_0' + F_2H_2' + 3F_0H_4' + 7H_4F_0' + 6F_1'F_3 + 5H_2F_2' + 4H_1F_3' + 3H_0F_4' + 2F_1H_3') = 0 \quad (14b)$$

$$F_4(0) = F_4'(0) = F_4'(\infty) = H_4'(0) = H_4(\infty) = 0 \quad (14c)$$

$$J_4'' + \frac{4}{5}(-J_4F_0'' + 2F_0'J_4' + 3F_0J_4'' + 2F_1J_3'' + 2J_3'F_1') + G_4 = \frac{6}{25}A_0 \cot\left(\frac{2\pi}{5}\right) \quad (15a)$$

$$G_4'' + \frac{4}{5}Pr(-J_4H_0' + 2F_1G_3' + 3F_0G_4' + 3H_0J_4' + 7G_4F_0' + 6G_3F_2' + 4H_1J_3') = 0 \quad (15b)$$

$$J_4(0) = J_4'(0) = J_4'(\infty) + \frac{2}{5}A_1 \cot\left(\frac{2\pi}{5}\right) = G_4'(0) = G_4(\infty) = 0 \quad (15c)$$

$$F_0(\eta) \sim A_0 \quad \text{as } \eta \rightarrow \infty \quad (16a)$$

$$F_1(\eta) \sim \frac{1}{4}\eta + A_1 \quad \text{as } \eta \rightarrow \infty \quad (16b)$$

$$J_3(\eta) \sim \frac{3}{5}A_0 \cot\left(\frac{2\pi}{5}\right)\eta + A_3 \quad \text{as } \eta \rightarrow \infty \quad (16c)$$

$$J_4(\eta) \sim -\frac{2}{5}A_1 \cot\left(\frac{2\pi}{5}\right)\eta + A_4 \quad \text{as } \eta \rightarrow \infty \quad (16d)$$

In the outer inviscid region,  $\bar{\psi}_0$  results merely from the presence of a free stream and is thus given by

$$\bar{\psi}_0 = U_\infty y = U_\infty r \sin \phi \quad (17)$$

where  $r$  is the radial distance from the source and  $\phi$  is the angular polar coordinate measured from the positive  $x$ -axis.

From matching considerations, the remaining terms of the outer expansion must satisfy

$$\nabla^2 \bar{\psi}_1 = 0 \quad (18a)$$

$$\bar{\psi}_1|_{\phi=0} = 4\nu A_0 \left(\frac{r}{D}\right)^{3/5}, \quad \bar{\psi}_1|_{\phi=\pi} = 0 \quad (18b)$$

$$\nabla^2 \bar{\psi}_2 = 0 \quad (19a)$$

$$\bar{\psi}_2|_{\phi=0} = 4\nu A_1 \bar{R} \left(\frac{r}{D}\right)^{2/5}, \quad \bar{\psi}_2|_{\phi=\pi} = 0 \quad (19b)$$

$$\nabla^2 \bar{\psi}_3 = 0 \quad (20a)$$

$$\bar{\psi}_3|_{\phi=0} = 4\nu A_2 \bar{R}^2 \left(\frac{r}{D}\right)^{1/5}, \quad \bar{\psi}_3|_{\phi=\pi} = 0 \quad (20b)$$

where

$$D = \left(\frac{g\beta N}{4\nu^2}\right)^{-5/12}, \quad A_2 = F_2(\infty). \quad (20c)$$

Solving equations (18a)–(20b), the outer expansion is obtained

$$\bar{\psi}_1 = 4\nu A_0 \left(\frac{r}{D}\right)^{3/5} \sin \frac{3(\pi-\phi)}{5} \left/ \sin \left(\frac{3\pi}{5}\right) \right. \quad (21)$$

$$\bar{\psi}_2 = 4\nu A_1 \bar{R} \left(\frac{r}{D}\right)^{2/5} \sin \frac{2(\pi-\phi)}{5} \left/ \sin \left(\frac{2\pi}{5}\right) \right. \quad (22)$$

$$\bar{\psi}_3 = 4\nu A_2 \bar{R}^2 \left(\frac{r}{D}\right)^{1/5} \sin \left(\frac{\pi-\phi}{5}\right) \left/ \sin \left(\frac{\pi}{5}\right) \right. \quad (23)$$

For the inner expansions, expressions (5) and (6) are not unique. To each of them may be added any one of an infinite set of eigen-solutions. Each of these satisfies a linear perturbation equation derived from equations (1) and (2) and also satisfies zero initial conditions and the condition of exponential decay at infinity. These eigenfunctions have the form  $(4\nu(Gr_\infty/4)^{1/4})C_n e_M^{\lambda_n} f_n(\eta)$  and  $\Delta T C_n e_M^{\lambda_n} \phi_n(\eta)$ , respectively. The constants  $C_n$ , indeterminate in general, are in some way associated with the stream function upstream,  $\lambda_n$  being the

corresponding eigenvalue. For the present problem the lowest order eigenfunctions associated with the inner expansions are given by

$$f_1 = 3F_0 - 2\eta F'_0 \quad (24a)$$

$$\phi_1 = 3H_0 + 2\eta H'_0 \quad (24b)$$

the eigenvalue  $\lambda_1$  is 5. As pointed out by Stewartson [8], an inconsistency arises in the large  $\eta$  behavior of the solution when a term in the postulated series is of the same order as one of the eigenfunctions. Such an inconsistency may be resolved by appropriately inserting a log or a log-log term into the series. However, having restricted ourselves to terms of  $O(\epsilon_M^4)$  in expansions (5) and (6), an inconsistency will not be encountered in the large  $\eta$  behavior of the solution as expressed in expansions (5) and (6). Thus, the assumed form of the solution in expansions (5) and (6) is appropriate to  $O(\epsilon_M^4)$ .

The total local convected energy downstream,  $Q(x)$ , defined in equation (4), now becomes, in view of expansions (5) and (6)

$$\begin{aligned} Q(x) = 8Pr \left( \frac{N^5 k^4 g \beta}{v^2} \right)^{1/4} \int_0^\infty \left\{ H_0 F'_0 + \epsilon_M (H_0 F'_1 \right. \\ + F'_0 H_1) + \epsilon_M^2 (F'_0 H_2 + H_1 F'_1 + H_0 F'_2) \\ + \epsilon_M^3 (F'_0 H_3 + F'_1 H_2 + F'_2 H_1 + H_0 F'_3) \\ + \epsilon_H (H_0 J'_3 + G_3 F'_0) + \epsilon_M^4 (H_0 F'_4 \\ + H_1 F'_3 + H_2 F'_2 + H_3 F'_1 + H_4 F'_0) \\ \left. + \epsilon_M \epsilon_H (H_0 J'_4 + F'_1 G_3 + F'_0 G_4) \right\} d\eta. \quad (25) \end{aligned}$$

However, using the energy equation of each level of expansion, it was determined that

$$\begin{aligned} Q(x) = 8Pr \left( \frac{N^5 k^4 g \beta}{v^2} \right)^{1/4} \left[ I_0 + \epsilon_M \left( \frac{5}{4Pr} H'_1(0) \right) \right. \\ + \epsilon_M^2 \left( \frac{5}{8Pr} H'_2(0) \right) + \epsilon_M^3 \left( \frac{5}{12Pr} H'_3(0) \right) \\ + \epsilon_H \left( \frac{5}{12Pr} G'_3(0) \right) + \epsilon_M^4 \left( \frac{5}{16Pr} H'_4(0) \right) \\ \left. + \epsilon_M \epsilon_H \left( \frac{5}{16Pr} G'_4(0) \right) \right]. \quad (26) \end{aligned}$$

Further simplification of the RHS of equation (26) is possible depending on the thermal condition imposed at the surface. Thus, for an adiabatic surface, higher order corrections to the surface temperature gradient, that is,  $H'_1(0)$ ,  $H'_2(0)$ , etc. must be zero. Then equation (26) simplifies to

$$Q(x) = 8Pr \left( \frac{N^5 k^4 g \beta}{v^2} \right)^{1/4} I_0 = \text{const.} \quad (27)$$

However, for a downstream temperature distribution which results in the surface being adiabatic to the zero order only, further simplification of equation (26) is not possible.

## RESULTS AND DISCUSSIONS

The inner region equations (9a)–(15c) were solved for  $Pr = 0.7$  and  $6.7$ . A modified predictor corrector method was used, supplemented by a shooting algorithm. Values of  $F''_i(0)$ ,  $i = 1, 2, 3, 4$ ;  $H_i(0)$ ,  $i = 2, 3, 4$ , and  $J''_3(0)$ ,  $J''_4(0)$ ,  $G_3(0)$ , and  $G_4(0)$  were guessed and subsequently corrected so as to eventually satisfy the far field boundary conditions. A fixed step size of  $\Delta\eta = 0.05$  was used in all calculations. The integration was performed from  $\eta = 0$  to  $\eta_{\text{edge}}$  which was taken to be 15 for  $Pr = 0.7$  and 30 for  $Pr = 6.7$ . The resulting values of  $F''_i(0)$ ,  $A_i$ ,  $i = 1, 2, 3, 4$ , and  $J''_3(0)$ ,  $J''_4(0)$ ,  $G_3(0)$ , and  $G_4(0)$  are gathered in Table 1. These results apply when the surface is adiabatic. Numerical solutions were also obtained for the circumstances in which downstream variation of the surface temperature is prescribed so that the surface is adiabatic to the zero order only. These results are also summarized in Table 2.

The velocity and temperature profiles determined as above are shown in Figs. 2–9. The effect of simultaneous inclusion of  $\epsilon_H$  and  $\epsilon_M$  is clear from Figs. 6–9. The presence of the  $\epsilon_H$  term in addition to the  $\epsilon_M$  term increases the velocity level in the flow. Thus the  $\epsilon_H$  term results in an effect similar to that of  $\epsilon_M$ . This question of similarity in the nature of these two effects is considered further, later. Also, for comparable values of  $\epsilon_M$  the effect of mixed convection is seen to be greater in air than in water.

Table 1. Computed constants for mixed convection flow from a wall plume, with the wall adiabatic

$i$	$F''_i(0)$	$Pr = 0.7$ $H_i(0)$	$A_i$	$F''_i(0)$	$Pr = 6.7$ $H_i(0)$	$A_i$
0	0.9297	1	0.8897	0.6575	1	0.4274
1	−0.0525	−0.1618	−0.5995	0.0023	−0.1028	0.6136
2	0.0176	−0.0015	0.0982	0.004	−0.0534	0.3350
3	0.0081	0.0132	−0.1869	0.0121	0.0599	−0.1084
4	−0.00067	−0.0022	−0.0808	−0.0010	−0.0035	−0.1740
	$J''_3(0) = -0.1004$			$J''_3(0) = -0.0139$		
	$J''_4(0) = -0.0791$			$J''_4(0) = -0.0235$		
	$G_3(0) = -0.3167$			$G_3(0) = -0.1232$		
	$G_4(0) = -0.1298$			$G_4(0) = -0.0725$		

Table 2. Computed constants for mixed convection flow from a wall plume, with a prescribed temperature variation on the wall

<i>i</i>	<i>Pr</i> = 0.7			<i>Pr</i> = 6.7		
	<i>F</i> <sub><i>i</i></sub> '(0)	<i>H</i> <sub><i>i</i></sub> '(0)	<i>A</i> <sub><i>i</i></sub>	<i>F</i> <sub><i>i</i></sub> '(0)	<i>H</i> <sub><i>i</i></sub> '(0)	<i>A</i> <sub><i>i</i></sub>
0	0.9297	0	0.8897	−0.6575	0	0.4274
1	0.1133	0.1056	−0.5090	0.0968	0.2238	−0.5747
2	0.2602	0.4371	0.4106	−0.0605	−0.4182	0.2984
3	−0.0605	−0.0543	−0.5730	0.0262	0.1443	−0.1521
4	−0.0116	−0.0567	−0.0234	0.0087	0.0126	−0.1651
	<i>J</i> <sub>3</sub> '(0) = −0.2054			<i>J</i> <sub>3</sub> '(0) = −0.0174		
	<i>J</i> <sub>4</sub> '(0) = −0.0278			<i>J</i> <sub>4</sub> '(0) = −0.0102		
	<i>G</i> <sub>3</sub> '(0) = −0.4878			<i>G</i> <sub>3</sub> '(0) = −0.2442		
	<i>G</i> <sub>4</sub> '(0) = −0.0907			<i>G</i> <sub>4</sub> '(0) = −0.0796		

The results (Table 1) reveal several subtle but very interesting aspects of mixed convection flows. For the adiabatic surface, it is seen that the first correction to the wall shear stress, the term of  $O(\epsilon_M)$  associated with  $F_1''(0)$ , is positive for  $Pr = 6.7$  and negative for  $Pr = 0.7$ . This is also clear from Figs. 2 and 4. Therefore, in air, increasing free stream velocity results in a decrease in the shear stress at the surface. From a physical standpoint this result for air at first appears to be wrong. For water  $F_1''(0) > 0$  and this apparent contradiction does not arise.

However, on probing deeper into the interactions of the underlying transport mechanisms, the reason for the apparently anomalous result, in air, becomes clear. At any location in the boundary region, the buoyancy

force tends to accelerate the fluid while the shear tends to decelerate it. When the ambient medium also has tangential momentum, an additional effect arises. As the ambient fluid is entrained into the boundary region, there will now be an additional contribution to the streamwise momentum. This, in turn, results in an increase in the velocity level near the edge of the velocity boundary region. This enhanced velocity level causes a reduction of the temperature level there. For an adiabatic surface condition, close to the surface, the temperature level is also reduced so that the surface remains adiabatic even to the first order. This results in reducing the buoyancy force near the surface. The extent of this reduction of buoyancy force near the surface is dictated by the extent of buoyancy force

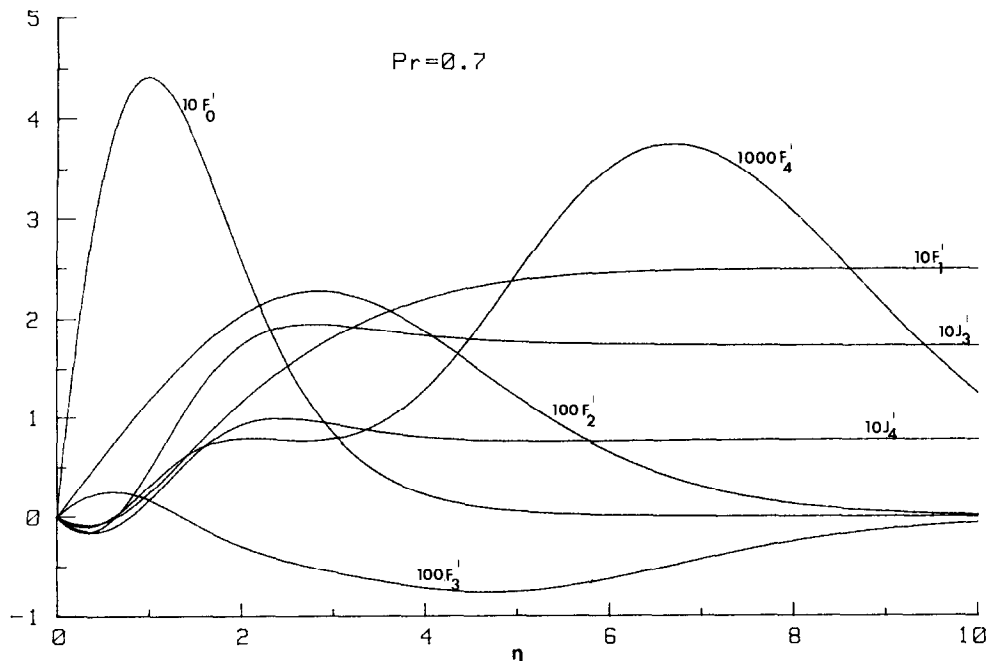


FIG. 2. Velocity function distributions for  $Pr = 0.7$ .

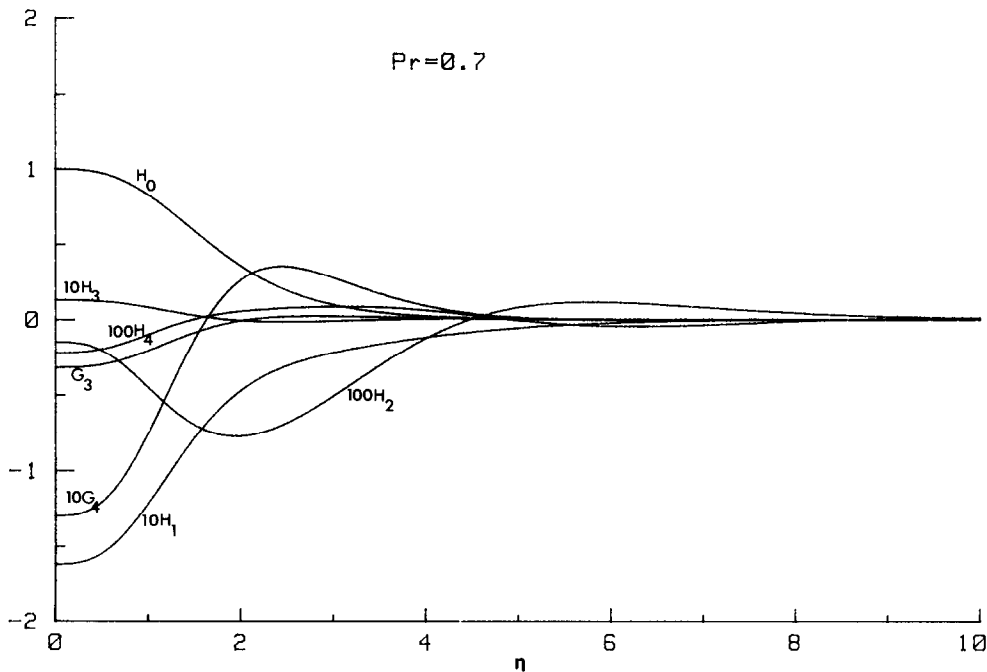


FIG. 3. Temperature function distributions for  $Pr = 0.7$ .

reduction near the edge of the thermal boundary layer. Thus, the buoyancy force is reduced everywhere in the thermal boundary layer, both in air and in water.

However, in air, the velocity and thermal boundary layers are of comparable magnitude whereas in water the former is relatively much thicker. In air, therefore, the buoyancy force is reduced across the entire

boundary region. In water the thermal boundary layer is embedded within the velocity boundary layer. Thus the full effect of the free stream velocity is felt by the thermal boundary layer, only in air. In water, the presence of a thicker velocity boundary layer, prevents the thermal boundary layer from seeing the full effect of the free stream velocity. This in turn results in a weaker

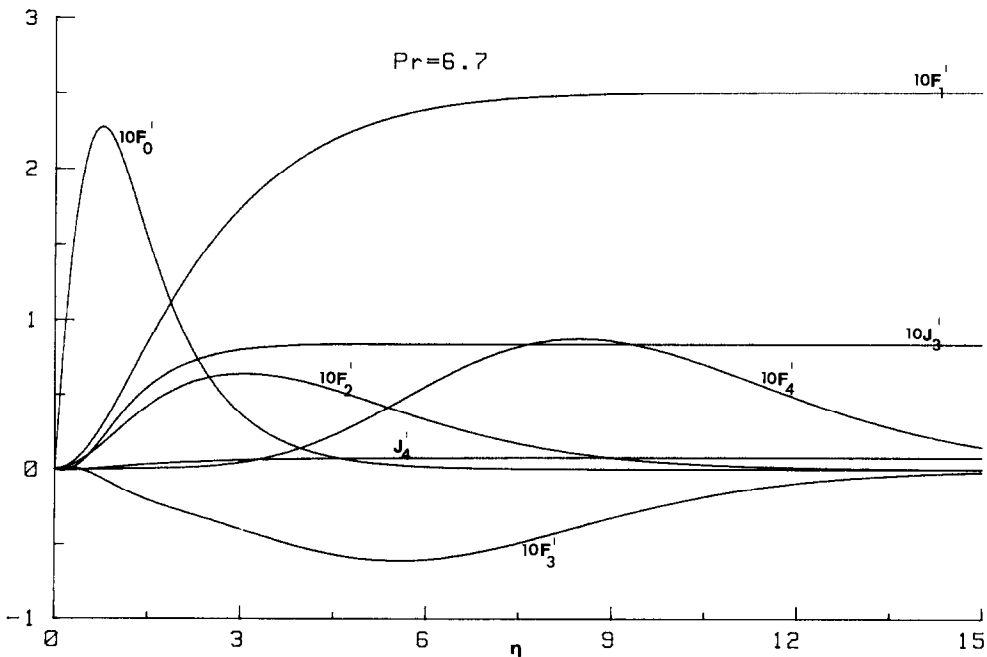


FIG. 4. Velocity function distributions for  $Pr = 6.7$ .

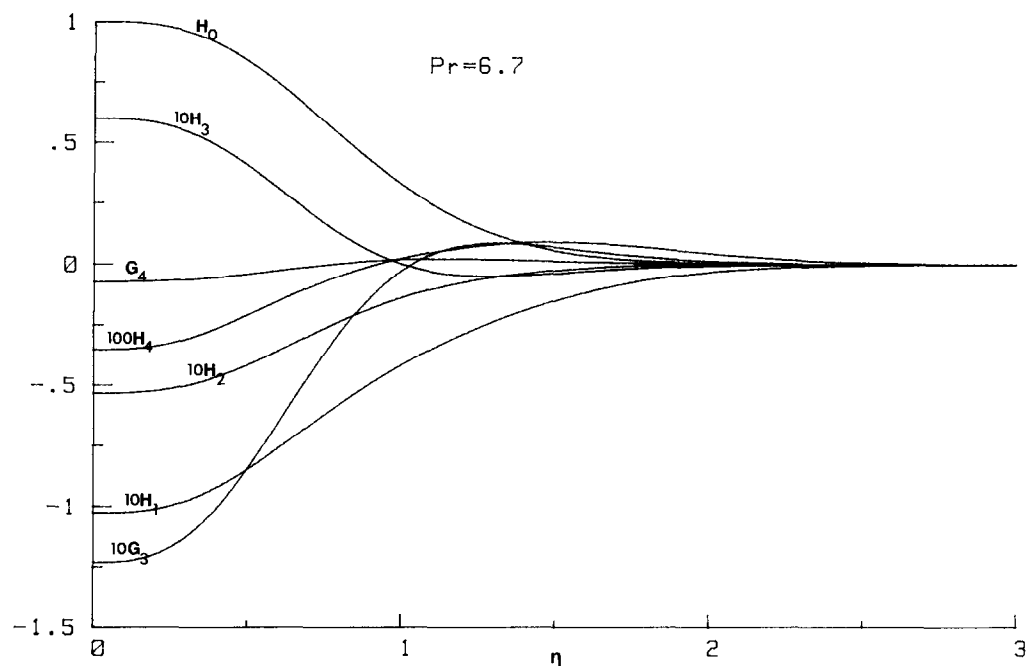


FIG. 5. Temperature function distributions for  $Pr = 6.7$ .

reduction of buoyancy force in water. Thus, in water, the buoyancy force, though reduced, is able to counteract the opposing shear stress, even near the surface, resulting in an overall increase in the velocity. Thus an increasing surface shear stress is found. The reduction in buoyancy force in air being greater, the buoyancy force is not strong enough to oppose the shear stress,

near the surface. The velocity near the surface is thereby lowered, resulting in a negative correction to the surface shear stress. Further calculations indicated that the transition from a positive correction of the wall shear stress to a negative one occurs close to  $Pr = 6$ .

The reduction of temperature level everywhere in the thermal boundary layer is central to the above

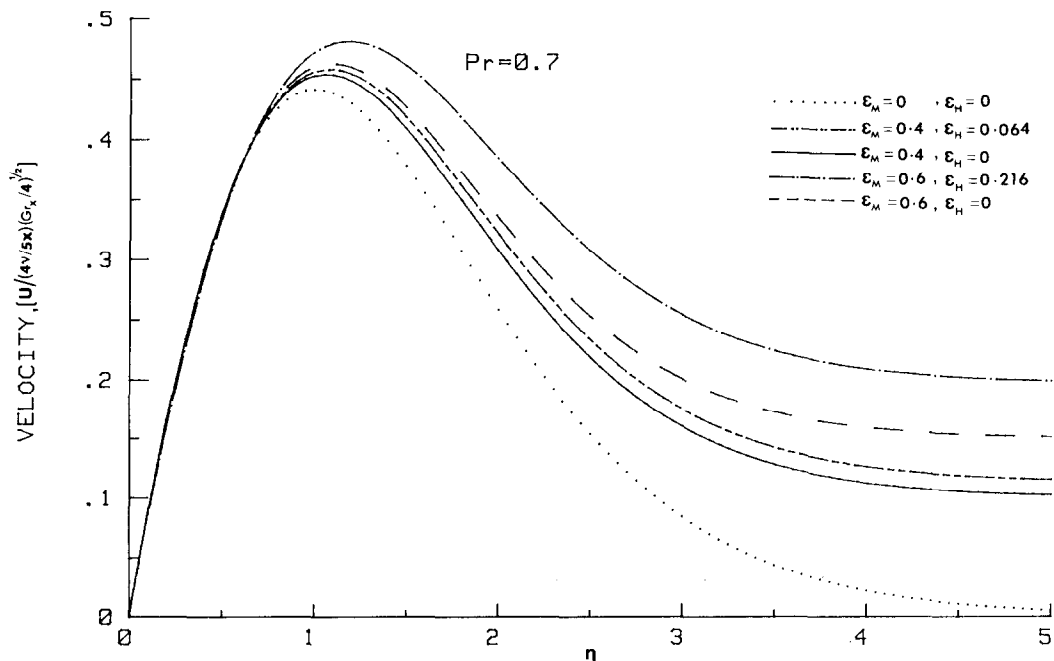


FIG. 6. Plot of velocity vs  $\eta$  for various values of  $\epsilon_M$  and  $\epsilon_H$  for  $Pr = 0.7$ .



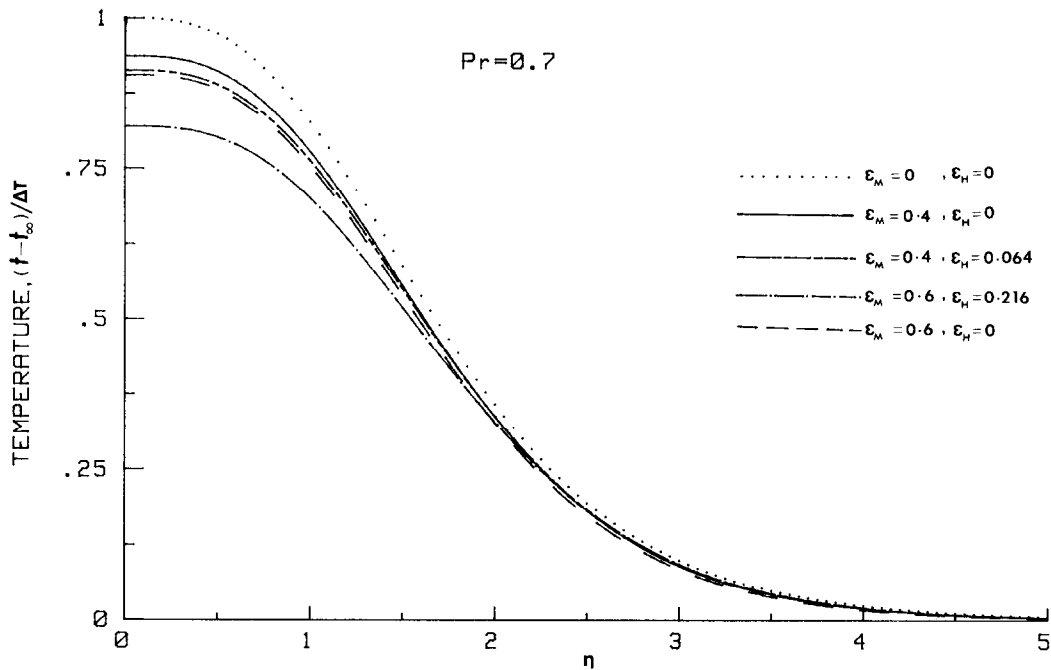


FIG. 7. Plot of temperature vs  $\eta$  for various values of  $\epsilon_M$  and  $\epsilon_H$  for  $Pr = 0.7$ .

interpretation. This reasoning for the transport near the surface resulted from the requirement that the surface be adiabatic. However, arguing on similar grounds it can be shown that whenever any flux condition is prescribed on the surface, the nature of corrections of  $O(\epsilon_M)$  to the surface shear stress will be identical to that described above. These same effects are

also evident in the results of Carey and Gebhart [5] for mixed convection from a uniform flux surface.

A question arises whether these effects would not arise if, instead, the surface temperature variation is prescribed. From Table 2 it is found that for both  $Pr = 0.7$  and  $6.7$ , the wall shear stress increases. The wall is not adiabatic in its interaction with the fluid

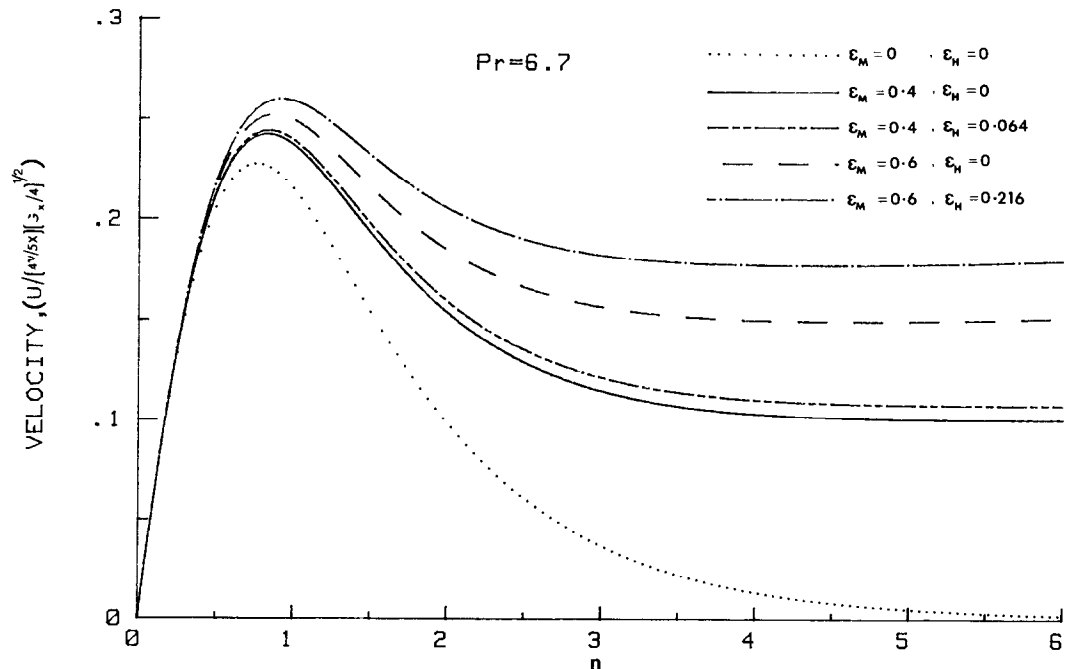


FIG. 8. Plot of velocity vs  $\eta$  for various values of  $\epsilon_M$  and  $\epsilon_H$  for  $Pr = 6.7$ .

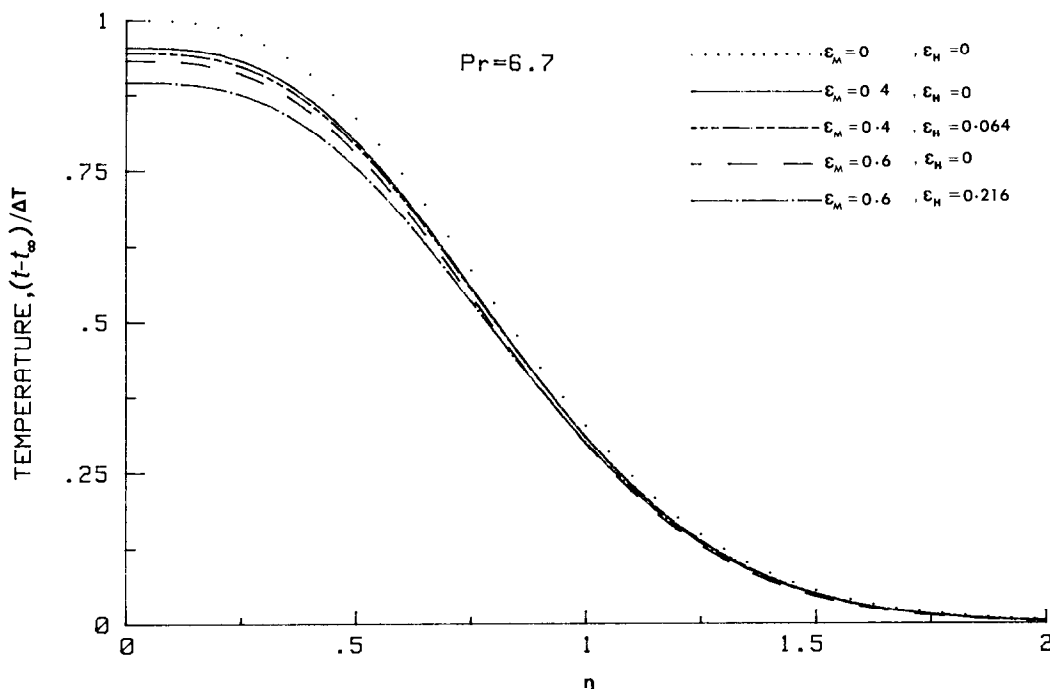


FIG. 9. Plot of temperature vs  $\eta$  for various values of  $\varepsilon_M$  and  $\varepsilon_H$  for  $Pr = 6.7$ .

and the temperature of the fluid near the surface does not decrease. Indeed, there is an overall increase in the temperature level near the surface, since  $H'_1(0)$  is positive. This increased buoyancy force opposes the shear stress and results in an increase in the velocity level. For an isothermal surface the same reasoning applies and the corrections at  $O(\varepsilon_M)$  to the shear stress and the heat flux at the wall are both positive. This is also reflected in the results of Merkin [9].

The terms  $J_3(\eta)$  and  $G_3(\eta)$  in equations (4) and (5), respectively, represent the non-boundary layer effects. At  $O(\varepsilon_H)$  they essentially account for the effects of the entrainment of ambient fluid at the edge of the boundary layer. The presence of entrainment results in a low velocity flow in the outer region. Thus, one might expect the effect of including these terms to be similar to that of mixed convection, described earlier. Based on the detailed arguments presented before we can conclude that the effect of mixed convection at  $O(\varepsilon_M)$  on the surface shear stress is strongly dependent on the thermal condition imposed at the surface and also on the Prandtl number. However, Tables 1 and 2 show that the corrections at  $O(\varepsilon_H)$  to the surface shear stress to be always negative. Thus the effects of these two parameters, that is  $\varepsilon_M$  and  $\varepsilon_H$ , appear to be governed by different mechanisms. In order to explain the nature of these corrections at  $O(\varepsilon_H)$  to the surface shear stress consider the contribution to  $Q(x)$  at  $O(\varepsilon_H)$ . See equation (25). Near the edge of the boundary layer the contribution to the integral is exponentially small since in this region both  $F_0$  and  $H_0$  decay exponentially to zero. However, in the middle part of the boundary region the contribution is positive as here,  $J'_3$ ,  $F_0$  and  $H_0$

are all positive. In order to offset this, both  $J'_3$  and  $G_3$  become negative close to the surface, so that finally the contribution to  $Q(x)$  at  $O(\varepsilon_H)$  remains zero.

## CONCLUSIONS

Consistent higher order approximations have been obtained for a mixed convection wall plume. A detailed explanation of the mechanisms involved has been provided, highlighting the subtle but interesting features of these flows. It is clearly established that the thermal condition at the surface exerts a strong influence on the wall shear stress. However, so far an experimental study of the circumstances considered here has not been reported in the literature. Also, the very complicated role played by the Prandtl number is clearly brought out. In conclusion, it is emphasized that non-boundary layer effects and mixed convection effects must be considered simultaneously and that they do not affect the flow in the same way.

*Acknowledgement*—The authors wish to acknowledge the support of this study by the National Science Foundation under the grant MEA 8200613.

## REFERENCES

1. V. D. Zimin and Y. N. Lyakhov, Convective wall plume, *J. Appl. Mech. Tech. Phys.* **11**, 159 (1970). Translated from Russian, January (1973).
2. Y. Jaluria and B. Gebhart, Buoyancy induced flow arising from a line thermal source on an adiabatic vertical surface, *Int. J. Heat Mass Transfer* **20**, 153 (1977).
3. N. Afzal, Convective wall plume: higher order analysis, *Int. J. Heat Mass Transfer* **23**, 505–513 (1980).

4. Y. Jaluria, Mixed convection in a wall plume, presented at the 20th Joint ASME/AIChE National Heat Transfer Conf., Milwaukee, Wisconsin, 2–5 August, 81-HT-37 (1981).
5. V. P. Carey and B. Gebhart, Transport at large downstream distances in mixed convection flow adjacent to a vertical uniform flux surface, *Int. J. Heat Mass Transfer* **25**, 255 (1982).
6. K. T. Yang and E. W. Jerger, First order perturbations of laminar free-convection boundary layers on a vertical plate *Trans. Am. Soc. Mech. Engrs, Series C, J. Heat Transfer* **86**, 107 (1964).
7. R. Krishnamurthy and B. Gebhart, Mixed convection from a line source plume, in press.
8. K. Stewartson, On asymptotic expansions in the theory of boundary layers, *J. Math. Phys.* **36**, 173 (1957).
9. J. H. Merkin, The effect of buoyancy forces on the boundary layer flow over a semi-infinite vertical flat plate in a uniform free stream, *J. Fluid Mech.* **35**, 439 (1969).

## CONVECTION MIXTE DANS LES PANACHES PARIETAUX

**Résumé**—On présente une analyse des effets de la convection mixte dans un écoulement de panache pariétal. Les résultats s'appliquent en aval de la source. La méthode de développement asymptotique est utilisée pour obtenir une solution en incluant à la fois les effets de la convection mixte et ceux des corrections de couche limite d'ordre élevé. Plusieurs configurations intéressantes de cet écoulement apparaissent et sont expliquées. Le rôle insoupçonné joué par les nombre de Prandtl est clairement illustré. Par exemple, l'effet d'un écoulement forcé favorable est de réduire le frottement pariétal pour  $Pr = 0,7$  et de l'augmenter pour  $Pr = 6,7$ . Il est montré aussi qu'un tel effet du nombre de Prandtl dépend des conditions de chauffage imposées à la paroi. On présente des résultats des calculs numériques pour deux nombres de Prandtl, 0,7 et 6,7 caractéristiques de l'air et de l'eau. L'effet global de la convection mixte sur la décroissance de la température de la surface et sur la valeur maximale de la vitesse tangentielle est plus important dans l'air que dans l'eau.

## ERZWUNGENE UND FREIE KONVEKTION BEI WANDAUFTRIEBSSTRÖMUNGEN

**Zusammenfassung**—Eine Untersuchung der kombinierten freien und erzwungenen Konvektion in einer Wandauftriebsströmung wird vorgestellt. Die Ergebnisse gelten stromabwärts von der Wärmequelle. Die Methode der angepassten asymptotischen Reihenentwicklung wurde verwendet, um eine konsistente Lösung zu erhalten, in welcher gleichzeitig die Einflüsse der kombinierten Konvektion und von Grenzschichtkorrekturen höherer Ordnung berücksichtigt sind. Mehrere subtile und interessante Eigenheiten dieser Strömung treten auf und werden erklärt. Die unerwartete Rolle, die die Prandtl-Zahl spielt, wird deutlich gemacht. So führt z. B. eine unterstützende erzwungene Konvektion bei  $Pr = 0,7$  zu einer Abnahme, bei  $Pr = 6,7$  zu einer Zunahme der Wandschubspannung. Weiter wird gezeigt, daß dieser Einfluß der Prandtl-Zahl auf die Wandschubspannung von der Art der Heizung abhängt, die der Wand aufgeprägt wird. Die Ergebnisse der numerischen Berechnungen werden für die Prandtl-Zahlen  $Pr = 0,7$  und  $6,7$ , charakteristisch für Luft und Wasser, dargestellt. Der Gesamteinfluß der kombinierten Konvektion auf die Abnahme der Wandtemperatur und auf das Maximum der tangentialen Geschwindigkeit ist bei Luft größer als bei Wasser.

## СМЕШАННАЯ КОНВЕКЦИЯ В СВОБОДНОКОНВЕКТИВНЫХ СТРУЯХ НА СТЕНКЕ

**Аннотация**—Представлен анализ эффектов смешанной конвекции при свободноконвективном струйном течении на стенке. Результаты справедливы для области вниз по потоку от источника. Для получения согласованного решения использован метод сращения асимптотических разложений, когда одновременно учитываются как эффекты смешанной конвекции, так и поправки высшего порядка для пограничного слоя. Отмечено несколько интересных особенностей такого течения и дано их толкование. Показана особая роль, которую играет число Прандтля. Например, совпадающий по направлению поток вынужденной конвекции снижает касательное напряжение на стенке при  $Pr = 0,7$  и увеличивает его при  $Pr = 6,7$ . Кроме того показано, что такое влияние числа Прандтля на касательное напряжение на стенке зависит от условий нагрева поверхности. Результаты численных расчетов представлены для двух значений числа Прандтля (0,7 и 6,7), характерных для воздуха и воды. Показано, что по сравнению с водой смешанная конвекция в воздухе оказывает большее влияние на снижение температуры поверхности вниз по течению и на максимальное значение тангенциальной скорости.